

# Structural, Spectroscopic and Theoretical Studies of <sup>t</sup>Butyl-isocyanide)gold(I) Iodide

Ruei-Yang Liao<sup>a</sup>, Trevor Mathieson<sup>a</sup>, Annette Schier<sup>a</sup>, Raphael J. F. Berger<sup>a</sup>, Nino Runeberg<sup>b</sup>, and Hubert Schmidbaur<sup>a</sup>

<sup>a</sup> Anorganisch-chemisches Institut der Technischen Universität München, Lichtenbergstrasse 4, D-85747 Garching, Germany

<sup>b</sup> Department of Chemistry, University of Helsinki, POB 55 (A. I. Virtasen aukio 1), FIN-00014 Helsinki, Finland

Reprint requests to Prof. Dr. Schmidbaur. E-mail: H.Schmidbaur@lrz.tum.de

Z. Naturforsch. **57 b**, 881–889 (2002); received June 3, 2002

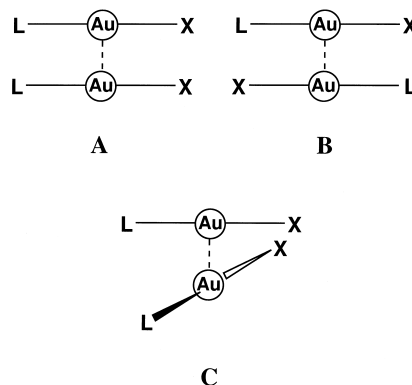
Isocyanide Complexes, Gold Complexes, Gold Iodide, Auophilicity

The complexes (<sup>t</sup>BuNC)AuCl and (<sup>t</sup>BuNC)AuI <sup>13</sup>C-labeled at the isocyanide group were prepared and investigated by concentration- and temperature-dependent IR and NMR spectroscopy in dichloromethane solution. No indication for association of the molecules was obtained. The crystal structure of the iodide complex was determined by X-ray diffraction methods and shown to feature only monomers with extremely large intermolecular Au–Au contacts of 4.162 Å, well beyond the sum of the van der Waals radii. It therefore appears that (<sup>t</sup>BuNC)AuI is a rare example of a sterically non-hindered L–Au–X complex which shows no auophilic interactions whatsoever. In a quantum-chemical analysis (at the local MP2 level) of the dimerization of the model compounds (MeNC)AuCl and (MeNC)AuI in various dimer geometries it was demonstrated that the energy-balance of the dimerization is very delicate and not dominated solely by contributions from correlation / relativistic (auophilic) effects.

## Introduction

Two-coordinate gold(I) complexes of the type L–Au–X are known to show association phenomena in the solid state [1] and under favourable conditions also in solution [2]. In the crystal this association leads to short intermolecular, sub-van-der-Waals contacts between the gold atoms in the range of d(Au–Au) 2.90 - 3.50 Å. This distance is dependent on a number of factors with main contributions from steric and electronic effects of the substituents (the neutral ligand L and the anionic ligand X) [3]. The geometry of the aggregates may vary from parallel (A) and antiparallel (B) to crossed / perpendicular dimers (C), and the energy associated with the aggregation has been measured [4] and calculated [5] to be in the order of 5 - 10 kcal/mole for a dimeric unit. However, the association can also be extended to give larger oligomers and one- or two-dimensional polymers [6]. The aggregation not only leads to interesting structures, but also to intriguing photophysical phenomena (absorption and luminescence spectra) [7]. In general terms, “auophilic” bonding of this type is now widely accepted as the

most prominent example of a more general phenomenon (“metallophilicity”) [6] and recognized as a major force determining supramolecular structures and properties [8].



While the effect is most obvious for most gold(I) complexes with tertiary amine, phosphine and arsine, as well as sulfide and selenide ligands (R<sub>3</sub>N, R<sub>3</sub>P, R<sub>3</sub>As, R<sub>2</sub>S, R<sub>2</sub>Se *etc.*), the isocyanide ligands RNC appear to weaken auophilic bonding as witnessed by exceedingly long intermolecular

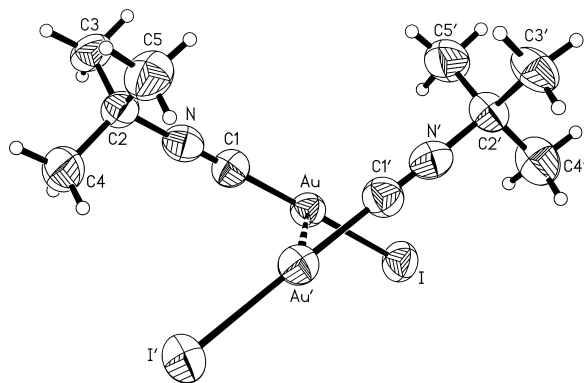


Fig. 1. X-ray structure of the dimeric subunits in  $C_5H_9AuIN$  (ORTEP [23] drawing, ellipsoids at the 50% probability level). The monomers are in a crossed orientation with a dihedral angle  $I-Au-Au'-I' = 108.8^\circ$  and an  $Au-Au'$  distance of  $4.612(3)$  Å. Selected monomer parameters:  $C1-Au = 1.95(1)$ ,  $Au-I = 2.513(1)$  Å and  $C(1)-Au-I = 177(1)^\circ$ .

$Au-Au$  contacts in crystals of compounds of the type  $(RNC)AuX$  [9]. Previous studies in this laboratory showed erratic results as the substituents  $R$  and  $X$  were changed from alkyl to aryl and ester, or from  $Cl$  to  $Br$ ,  $I$ ,  $NO_3$  etc., respectively [10 - 14]. Contrary to expectations based on previously proposed rules [3, 5], the combination isocyanide/iodide - both extremely soft donors - seemed to lead to particularly poor interactions. In order to clarify this point, the title iodine compound was investigated in detail now, following work on the corresponding chloro and bromo analogues.  $(^tBuNC)AuCl$  and  $(^tBuNC)AuBr$  are isomorphous and form chain structures with rather long  $Au-Au$  distances of  $3.695(1)$  and  $3.689(1)$  Å, respectively [10]. Along these chains, neighbouring molecules are arranged antiparallel head-to-tail, but the molecules are shifted against each other in such a way that the  $Au-Au$  contacts are not the minimum distance between the molecules. These shifts also indicate very weak - if any -  $Au-Au$  bonding.

### Preparations

(*t*-Butyl-isocyanide)gold(I) iodide was prepared from the corresponding chloride [10] by metathesis reaction with potassium iodide in a dichloromethane / water two-phase system. The product was isolated from the organic phase as a colorless microcrystalline material in 70% yield. Protection of the reaction vessel against incandescent light is re-

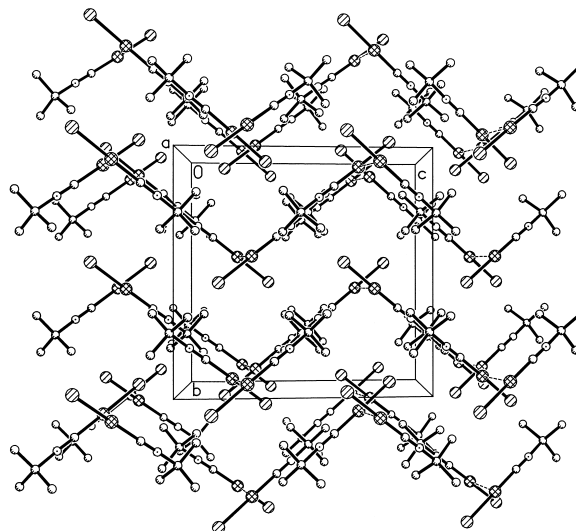


Fig. 2. Projection onto the  $bc$  plane in the x-ray structure of  $C_5H_9AuIN$ . All  $I-I$  distances are well beyond  $4.50$  Å. The structure can be considered to be a space-filling array of monomers with no indication for discrete aurophilic ( $Au-Au$ ) or other closed-shell interactions ( $I-I$ ,  $Au-I$ ).

quired to avoid decomposition. Single crystals of  $(^tBuNC)AuI$  were grown from dichloromethane / pentane.

For the spectroscopic studies, the compound with  $^{13}C$ -enrichment at the isocyanide function was also synthesized. For this purpose,  $^tBuN^{13}C$  was generated from  $^{13}CHCl_3 / ^{12}CHCl_3$  (7%  $^{13}C$ ),  $^tBuNH_2$  and  $NaOH$  in the presence of  $[Et_3NBz]Cl$  in a dichloromethane / water two-phase system at reflux temperature. The product was isolated as a colorless liquid by fractional distillation in 66% yield.

From this carbon-labeled isocyanide the  $AuCl$  complex was prepared using (tetrahydrothiophene)gold chloride as the substrate. The resulting labeled chloride (7%  $^{13}C$ , 80% yield) was then converted into the labeled iodide (7%  $^{13}C$ , 70% yield) following the above procedure.

### Crystal Structure

Crystals of  $(^tBuNC)AuI$  are monoclinic, space group  $C2/c$ , with  $Z = 8$  formula units in the unit cell. The molecules are arranged in pairs with the components related by a twofold axis (Fig. 1). The shortest distance between the monomers is between the two gold atoms, but the  $Au-Au'$  distance is  $4.162$  Å indicating that this is at best a weak van-der-Waals contact. The structure of the monomer is a linear array

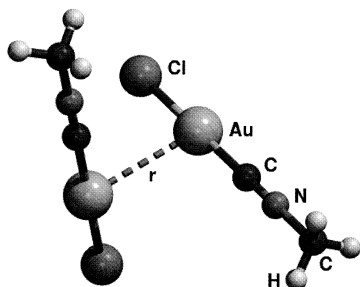


Fig. 3. The structure of the  $(\text{H}_3\text{CNCAuX})_2$  model dimer.

of five atoms (I-Au-C-N-C) with standard distances and angles: Au-C1 1.95(1), Au-I 2.513(1), C1-N1 1.13(1), C2-N1 1.47(2) Å; I-Au-C1 178.7(4)°, N1-C1-Au 179(1)°, C1-N1-C2 177(1)°. The monomers are in a crossed orientation with a dihedral angle I-Au-Au'-I' = 108.8° (Fig. 1).

Projections of the unit cell along its axes shows that there are no conspicuously short contacts between the iodine atoms of the molecules. (Fig. 2 shows a projection onto the bc plane). In fact all intermolecular I-I distances are well beyond 4.50 Å. The crystal structure thus can be considered to be a space-filing array of monomers with no indication for discrete aurophilic (Au-Au) or other closed-shell interactions (I-I, Au-I).

### Spectroscopic Studies

Solutions of (*t*-BuN<sup>13</sup>C)AuI in dichloromethane-d<sub>2</sub> show three <sup>13</sup>C NMR signals at 29.8 (s, Me), 59.4 (s, Me<sub>3</sub>C) and 143.2 [t,  $J(^{14}\text{N}-^{13}\text{C}) = 21.9$  Hz, NC]. The corresponding data for (*t*-BuNC)AuCl are 29.83 (s, Me), 59.60 [t,  $J(^{14}\text{N}-^{13}\text{C}) = 4.1$  Hz, Me<sub>3</sub>C] and

132.49 (t,  $J = 24.2$  Hz, NC). Both spectra are largely independent of concentration (0.20 - 0.65 mole/l for the chloride, 0.3 - 1.0 mole/l for the iodide) and temperature (-80 - +20 °C). The small shifts with concentration and temperature are all close to the standard deviations of the experiments. The resonances of (*t*-BuNC)AuI become broad at low temperature (-60 °C) and the <sup>14</sup>N-<sup>13</sup>C coupling is lost. This result may be ascribed to a ligand redistribution involving ionic isomers or to a reduced fluctuation in the solvation which generates a change in the electric field gradient at the quadrupolar nuclei (<sup>14</sup>N, <sup>197</sup>Au) and a change in relaxation times. Therefore there is no indication for oligomerization of (*t*-butylisocyanide)gold iodide in solution.

### Computational Part

The solid state structure of *t*-BuNCAuI (above) shows exceedingly long intermolecular Au-Au distances (4.16 Å). It is thus a particularly striking example that solid state structures of Au(I) isocyanide complexes show in general very long intermolecular Au-Au contacts. The result prompts the question: "Is this an intrinsic electronic effect induced by the isonitrile ligand?" In an attempt to answer this question we studied methylisonitrile gold(I) chloride and iodide dimers {[MeNCAuX]<sub>2</sub>, X = (Cl, I)} by quantum-chemical methods in the gas phase as model systems and compared the results of these calculations with previous computational data on the analogous phosphine systems {[H<sub>3</sub>PAuX]<sub>2</sub>, X = (H, F, Cl, Br, I, -CN, -CH<sub>3</sub>, -SCH<sub>3</sub>)} [3].

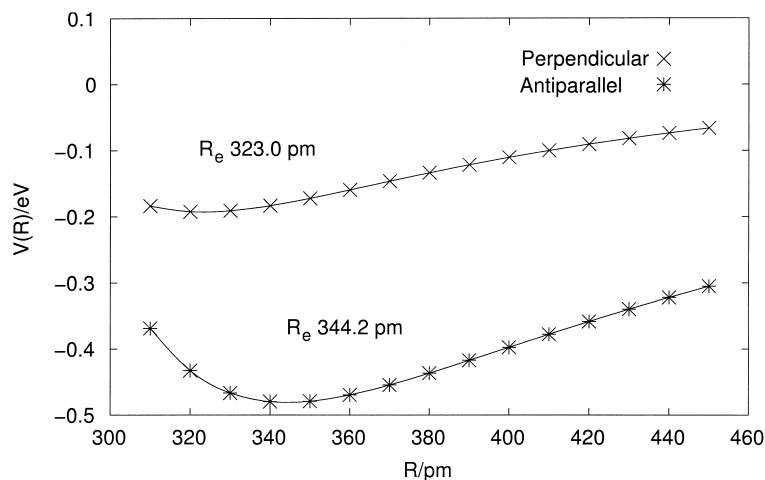


Fig. 4. The calculated interaction energy of the  $(\text{MeNCAuCl})_2$  dimer in perpendicular ( $\theta = 90^\circ$ ) and antiparallel ( $\theta = 180^\circ$ ) arrangement at LMP2/AVDZ level of theory.

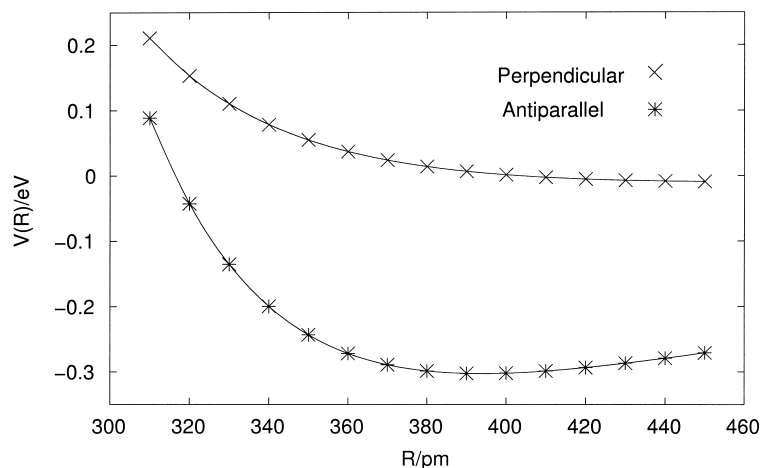


Fig. 5. The calculated interaction energy of the  $(\text{MeNCAuCl})_2$  dimer in perpendicular ( $\theta = 90^\circ$ ) and antiparallel ( $\theta = 180^\circ$ ) arrangement at SCF/AVDZ level of theory.

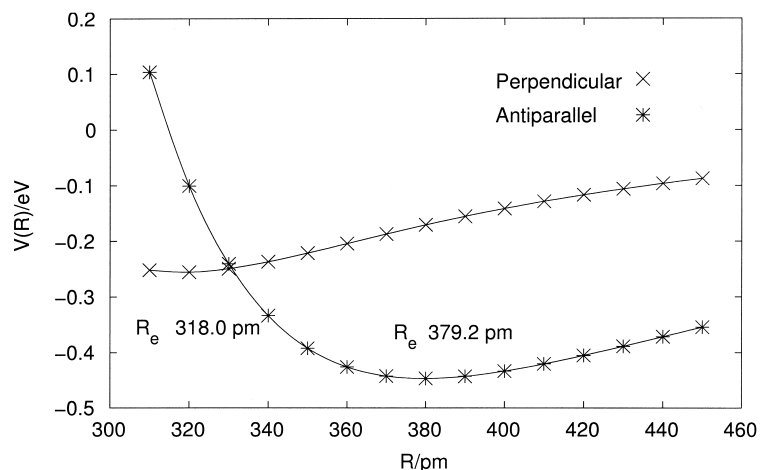


Fig. 6. The calculated interaction energy of the  $(\text{MeNCAuI})_2$  dimer in perpendicular ( $\theta = 90^\circ$ ) and antiparallel ( $\theta = 180^\circ$ ) arrangement at LMP2/AVDZ level of theory.

In calculations of the dimers the monomers were aligned to produce XAuAu angles of  $90^\circ$ . The optimized monomer structures and the dihedral angle [ $\theta = 90^\circ$  (perpendicular arrangement)] were frozen and only the Au-Au distance was changed (see Fig. 3).

At LMP2 level (local-MP2, see Computational Details) the Au-Au equilibrium distance of the  $(\text{MeNCAuCl})_2$  dimer is found to be  $3.230 \text{ \AA}$ , and the corresponding interaction energy is  $19 \text{ kJ/mol}$  (see Fig. 4, perpendicular arrangement).

At SCF level the intermolecular potential appears to be purely repulsive (see Fig. 5, perpendicular arrangement), which is as expected, since aurophilic attractions are basically dispersion interactions, which can only be described in terms of electronic correlation.

For the  $(\text{MeNCAuI})_2$  dimer the Au-Au equilibrium distance is  $3.180 \text{ \AA}$  and the interaction energy is  $25 \text{ kJ/mol}$  at LMP2 level (see Fig. 6, perpendicular arrangement).

SCF methods again yield a repulsive potential without any local minima for the  $(\text{MeNCAuI})_2$  dimer (see Fig. 7).

Table 1 shows the results together with the corresponding values calculated for the phosphine complexes [3]. Firstly the comparison suggests, that there is no principal difference in interaction *energies* between isonitrile and phosphine complexes within computational accuracy (at least  $\pm 5 \text{ kJ/mol}$ ). Secondly the interaction energy when changing from the harder chloride to the softer iodide is not only increasing in case of the phosphine ligand [3] but also for the isonitrile ligand. Thirdly and most

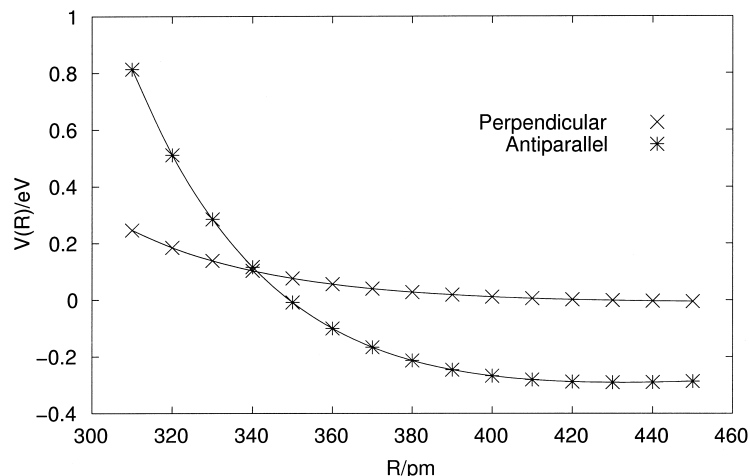


Fig. 7. The calculated interaction energy of the  $(\text{MeNCAuI})_2$  dimer in perpendicular ( $\Theta = 90^\circ$ ) and antiparallel ( $\Theta = 180^\circ$ ) arrangement at SCF/AVDZ level of theory.

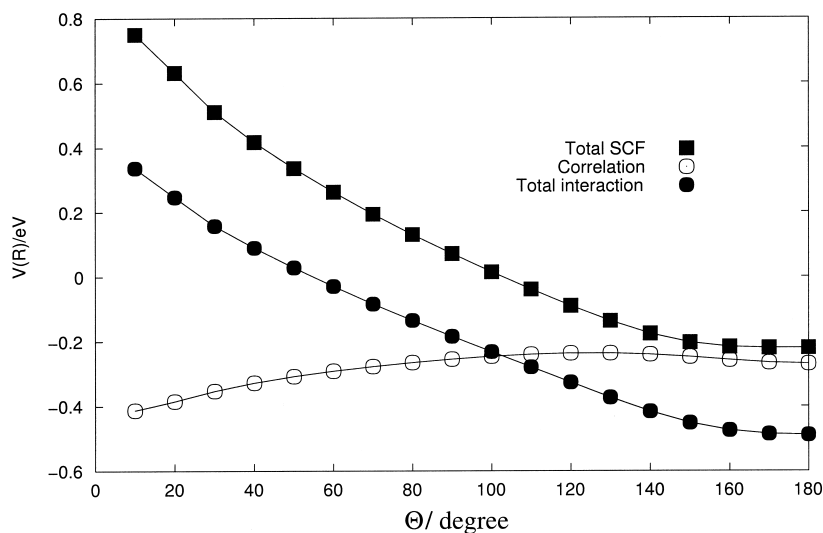


Fig. 8. The calculated interaction energy of the  $(\text{MeNCAuCl})_2$  dimer at a fixed Au-Au distance of 3.442 Å and different torsion angles  $\Theta$  (LMP2 / AVDZ level of theory).

Table 1. Equilibrium distances and interaction energies of  $(\text{LAuX})_2$  ( $L = \text{MeNC}, \text{H}_3\text{P}$ ;  $X = \text{Cl}, \text{I}$ ) dimers in perpendicular arrangement ( $\Theta = 90^\circ$ ) calculated at second-order-perturbation-theory levels.

Molecule	$R_e$ [Å]	$\Delta E$ [kJ/mol]
$(\text{H}_3\text{PAuCl})_2$ [3]	3.366	17
$(\text{MeNCAuCl})_2$	3.230	19
$(\text{H}_3\text{PAuI})_2$ [3]	3.315	23
$(\text{MeNCAuI})_2$	3.180	25

surprising, the isocyanide complexes have *shorter* Au-Au contacts in these model systems. Since this is clearly in contrast to the experimental observations, attempts were made to refine the model.

Table 2. Equilibrium distances and interaction energies of  $(\text{MeAuX})_2$  ( $X = \text{Cl}, \text{I}$ ) dimers in antiparallel arrangement ( $\Theta = 180^\circ$ ) calculated at LMP2/AVDZ level of theory.

Molecule	$R_e$ [Å]	$\Delta E$ [kJ/mol]
$(\text{MeNCAuCl})_2$	3.442	47
$(\text{MeNCAuI})_2$	3.792	41

Loosening the restraint of a  $90^\circ$  torsion angle  $\Theta$  yields an Au-Au distance of 3.442 Å for the chloride and of 3.792 Å for the iodide, with a torsion angle at equilibrium of  $180^\circ$  (= antiparallel configuration) in both cases (see Fig. 8). The dimerization energies for these configurations are 47 kJ/mol and 41 kJ/mol for the chloride and iodide, respectively

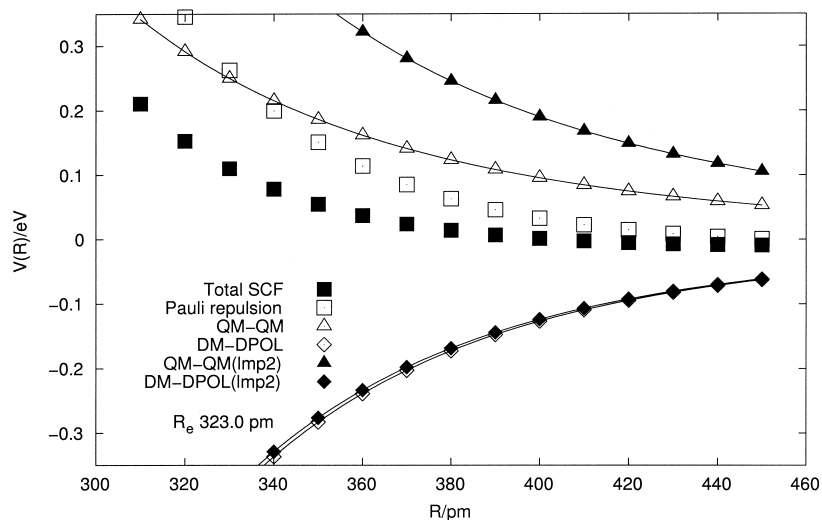


Fig. 9. The calculated LMP2 / AVDZ interaction potential contributions of the perpendicular ( $\text{MeNCAuCl}$ )<sub>2</sub> dimer partitioned according to equations 1 - 3. The (LMP2) labels correspond to results obtained by using the LMP2 values.

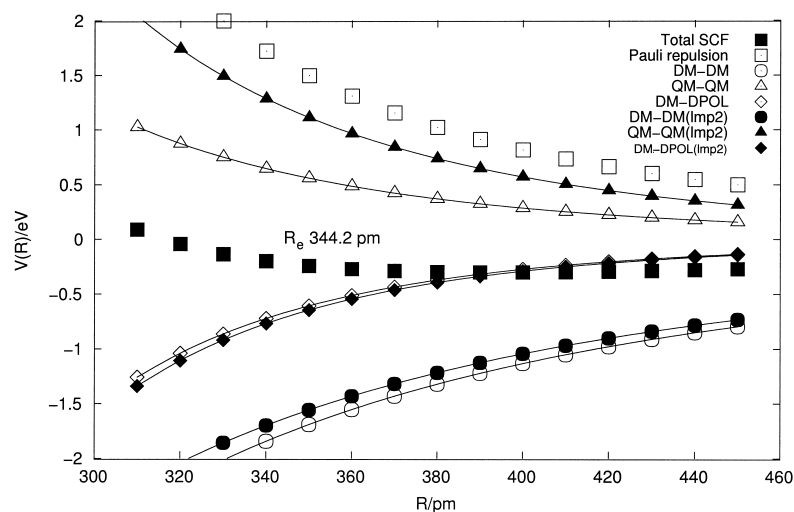


Fig. 10. The calculated LMP2 / AVDZ interaction energy of the antiparallel ( $\text{MeNCAuCl}$ )<sub>2</sub> dimer partitioned according to equations 1 - 3. The (LMP2) labels correspond to results obtained by using the LMP2 values for the properties.

(Table 2, Figs. 4, 6). Surprisingly, the SCF potential for the antiparallel ( $\text{MeNCAuCl}$ )<sub>2</sub> dimer is no more repulsive and shows a local minimum at about 3.95 Å, while for the ( $\text{MeNCAuI}$ )<sub>2</sub> it is flat for all  $R$  values larger than 4.20 Å. The result is a much *higher* total (LMP2) dimer stabilisation energy at an antiparallel arrangement, but at a *longer* intermolecular distance.

To make the situation more transparent, an energy contribution analysis in terms of classical electrostatic potentials (see Computational Details) was carried out for the perpendicular and the antiparallel equilibrium geometry of the ( $\text{MeNCAuCl}$ )<sub>2</sub> dimer (see Figs. 9 and 10). The major repulsive

contribution in the antiparallel case is the short range “Pauli” repulsion, followed by a quadrupole-quadrupole interaction, while the major attractive contribution is represented by the dipole-dipole interaction, followed by dipole-induced-dipole interactions. In summary, these contributions yield a slightly *repulsive* (SCF) potential.

In contrast to the antiparallel case, the major repulsive contribution in the perpendicular configuration is no longer the *very short* range “Pauli” repulsion but rather the somewhat more long ranging quadrupole-quadrupole interaction, and the major attractive contribution in this case is the dipole-induced-dipole interaction. In classical elec-

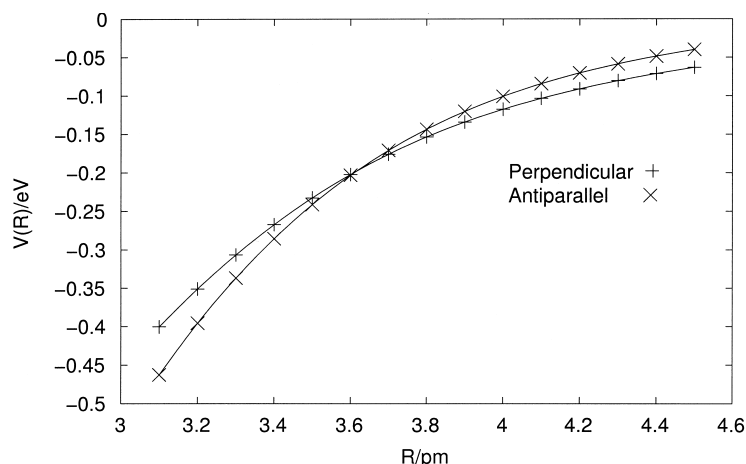


Fig. 11. The calculated LMP2/AVDZ correlation energy of  $(\text{MeNCAuCl})_2$  dimer in parallel and antiparallel orientation.

trostatic terms again a repulsive SCF potential is obtained.

It is only the correlation energy, which is responsible for the main part of the aurophilic interaction and leads in both cases (parallel and antiparallel configuration) to a potential curve with a distinct local minimum. Since the correlation energy contribution is largely the same for the antiparallel and the perpendicular case (see Fig. 8), the difference in the potential curves between the parallel and the perpendicular configuration is only determined by the classical electrostatic contributions. In other words: Aurophilic attraction is a necessary but not commensurate condition for the structure of the dimers.

Electron correlation energies are the smallest contributions of the total energy of the dimers for the antiparallel arrangement and are in the same order of magnitude as the dipole-induced-dipole interaction energies for the perpendicular arrangement (see Fig. 11)].

### Conclusion

The strong monomer-monomer interaction at a relatively large distance in  $(\text{RNC})\text{AuX}$  dimers with antiparallel orientation of monomers is mainly a result of the dominating long-range dipole-dipole attraction and the short-range steric (“Pauli”) repulsion. The short but only weak monomer-monomer interaction in the perpendicular case is a result of the less dominating steric repulsion and the dipole-induced dipole attraction, which is weaker than the dipole-dipole attraction of the antiparallel case. The necessary condition to make these effects experi-

mentally observable is an aurophilic correlation attraction, which is not significantly influenced by the type of ligands (methylisonitrile and phosphine).

### Computational Details

In the present work the interaction energies of the  $(\text{MeNCAuX})_2$  ( $X = \text{Cl}, \text{I}$ ) dimers were studied for various structural combinations of the monomers. All calculations were performed at the local MP2 (LMP2) level, as implemented in the MOLPRO programme package [15]. The basis sets are of polarized valence double-zeta (VDZP) quality, comprising an energy-consistent 19 valence-electron (VE) quasirelativistic pseudopotential (QRPP) with an  $(8s7p6d2f) / [7s6p3d2f]$  valence basis set on gold [16, 17], a 8-VE QRPP with a  $(4s4p1d)$  basis on I [18, 19] and all-electron basis sets for H, C, N and Cl [20, 21].

The LMP2 method introduces some conceptual advantages for studying intermolecular interactions, such as a drastically reduced basis-set superposition error (BSSE) and the possibility to decompose the correlation energy into physically meaningful contributions [15].

The Au  $5s5p$ , the Cl  $1s2s2p$  as well as the  $1s$  electrons on C and N were excluded from the correlational treatment. The optimized structural parameters of the monomers are given in Table 3. Some important physical properties are compiled in Table 4.

The energy of the two interacting linear polar molecules is dominated by the following non-vanishing components: The short range “Pauli” re-

Table 3. At LMP2/AVDZ level optimized parameters of the MeNCAuX (X = Cl, I) monomers. Bond lengths in Å, angles in degrees.

	MeNCAuX X = Cl			MeNCAuX X = I	
	X = Cl	X = I		X = Cl	X = I
X-Au	2.26	2.56	Au-C	1.90	1.93
C-N	1.18	1.18	N-C	1.43	1.43
C-H	1.09	1.09			
X-Au-C	180	180	Au-C-N	180	180
C-N-C	180	180	N-C-H	109	109

Table 4. Calculated dipole moment ( $\mu$ ), quadrupole moment ( $\omega$ ) and dipole polarizability [parallel ( $\alpha_{\parallel}$ ) and perpendicular ( $\alpha_{\perp}$ )] components of the MeNCAuX (X = Cl, I) monomers in au.

Method	$\mu$	$\omega$	$\alpha_{\parallel}$	$\alpha_{\perp}$
<i>MeNCAuCl:</i>				
SCF	4.24	10.75	103.99	48.40
LMP2	4.07	15.16	120.13	51.31
<i>MeNCAuI:</i>				
SCF	4.41	22.21	144.60	63.91
LMP2	4.18	26.42	162.83	65.33

pulsion ( $V_{\text{short}}$ ), dipole-dipole interaction ( $V_{\text{dm-dm}}$ ), quadrupole-quadrupole interaction ( $V_{\text{qm-qm}}$ ), inductive dipole-polarizability interaction ( $V_{\text{dm-pol}}$ ), and the dispersion due to interaction between the dipole polarizabilities ( $V_{\text{disp}}$ ). The classical expressions for  $V_{\text{dm-dm}}$ ,  $V_{\text{qm-qm}}$  and  $V_{\text{dm-pol}}$  of two identical, linear polar molecules are

$$V_{\text{dm-dm}} = \frac{\mu}{R^3} \cos(\Theta), \quad (1)$$

$$V_{\text{qm-qm}} = \frac{3\omega^2}{4R^5} (1 + 2 \cos(\Theta)), \quad (2)$$

$$V_{\text{dm-pol}} = -\frac{\alpha\mu^2}{R^6} + \frac{(\alpha_{\parallel} - \alpha_{\perp})\mu^2}{R^6} (3 \cos^2(\Theta) - 1). \quad (3)$$

## Experimental Part

### Preparation of <sup>13</sup>C-labeled <sup>t</sup>Butylisocyanide

Following a literature procedure [22] the isonitrile was prepared from <sup>t</sup>butylamine (26 ml, 17.94 g, 0.241 mmol), chloroform-<sup>13</sup>C (0.667 ml, 1.0 g, 8.27 mmol), chloroform-<sup>12</sup>C (9 ml, 13.5 g, 0.113 mol), and benzyl-triethylammonium chloride (0.25 g) in 37.5 ml of dichloromethane, and sodium hydroxide (37.5 g, 0.938 mol) in 40 ml of water. After 4 h of reflux with stirring and cooling to 20 °C ice

water (100 ml) is added to the reaction mixture. The aqueous phase is extracted with dichloromethane (12.5 ml) and the combined organic phase is washed with water (12.5 ml) followed by 12.5 ml of 5% [w/w] of aqueous sodium chloride solution. The solution is dried over MgSO<sub>4</sub> and distilled under nitrogen; b. p. 85 °C, 6.65 g yield (66%). NMR (CDCl<sub>3</sub>, 20 °C), <sup>13</sup>C{<sup>1</sup>H}: 30.65, s, Me; 54.08, t, *J* 5.3 Hz, CMe<sub>3</sub>; 152.47, t, *J* 8.8 Hz, CN. IR (liquid film): 2137.4 cm<sup>-1</sup>.

### Preparation of <sup>13</sup>C-labeled (<sup>t</sup>butylisocyanide)gold(I) chloride and iodide

0.468 g of <sup>t</sup>BuNC (0.64 ml, 5.63 mmol) and (tetrahydrothiophen)gold(I) chloride (1.80 g, 5.63 mmol) are dissolved in dichloromethane (40 ml) at 20 °C under nitrogen [10]. After 1 h of stirring a clear solution is obtained. The volume of this solution is reduced to 2 ml in a vacuum to precipitate the product, which is filtered and dried in a vacuum: 1.41 g yield (80%). NMR (CD<sub>2</sub>Cl<sub>2</sub>, 20 °C), <sup>13</sup>C{<sup>1</sup>H}: 29.83, s, Me; 59.60, t, *J* 4.0 Hz, CMe<sub>3</sub>; 132.49, t, *J* 24.2 Hz, AuC.

0.7 g of (<sup>t</sup>BuNC)AuCl (2.22 mmol) is dissolved in dichloromethane (10 ml) and treated with a solution of KI (0.366 g, 2.22 mmol) in water (10 ml). The mixture is stirred at 0 °C for 3 h under nitrogen and with protection against light. The phases are separated, the aqueous phase is washed with dichloromethane (2 × 5 ml) and the combined organic phase is washed with water (2 × 5 ml), dried over MgSO<sub>4</sub> and evaporated to dryness in a vacuum: 0.6 g yield (70%), m. p. 85 °C. NMR (CD<sub>2</sub>Cl<sub>2</sub>, 20 °C) <sup>1</sup>H: 1.54, s, Me. <sup>13</sup>C{<sup>1</sup>H}: 29.72, s, Me; 59.19, s, CMe<sub>3</sub>; 142.48, t, *J* 21.9 Hz, AuC. IR (KBr): 2239.2 cm<sup>-1</sup> (CN); IR (Nujol): 2235.8 cm<sup>-1</sup>. C<sub>3</sub>H<sub>9</sub>NAuI (406.99) calcd. C 14.76, H 2.23, N 3.44; found C 15.07, H 2.28, N 3.52. – MS(Cl): *m/z* = 406.7 (3%) [M<sup>+</sup>].

### Crystal structure analysis

The crystalline sample was placed in inert oil, mounted on a glass pin, and transferred to the cold gas stream of the diffractometer. Crystal data were collected and integrated using an Enraf Nonius CAD4 system with monochromated Mo-K<sub>α</sub> ( $\lambda = 0.71073$  Å) radiation at –50 °C. The structure was solved by a combination of direct methods and difference-Fourier syntheses and refined by full matrix least-squares calculations on  $F^2$ . The thermal motion was treated anisotropically for all non-hydrogen atoms. All hydrogen atoms were calculated and allowed to ride on their corresponding C atoms with fixed isotropic contributions.

*Crystal data for C<sub>3</sub>H<sub>9</sub>AuIN*:  $M_r = 407.0$ , colourless crystal, monoclinic,  $a = 12.413(2)$ ,  $b = 11.977(1)$ ,  $c = 12.448(2)$  Å,  $\beta = 97.68(2)^\circ$ , space group  $C2/c$ ,  $Z = 8$ ,  $V =$



1834.0(4) Å<sup>3</sup>,  $\rho_{calc} = 2.948 \text{ g cm}^{-3}$ ,  $F(000) = 1424$ ; 2501 measured and 1973 unique reflections [ $R_{int} = 0.0547$ ]; 73 refined parameters,  $wR2 = 0.1142$ ,  $R1 = 0.0473$ . Residual electron densities:  $+2.151 / -1.279 \text{ e/Å}^3$ . The function minimized was:  $wR2 = \{[\sum w(F_o^2 - F_c^2)^2] / \sum [w(F_o^2)^2]\}^{1/2}$ ;  $w = 1 / [\sigma^2(F_o^2) + (ap)^2 + bp]$ ;  $p = (F_o^2 + 2F_c^2) / 3$ ;  $a = 0.0676$ ,  $b = 0.00$ . Selected interatomic distances and angles are given in the corresponding figure caption. Anisotropic thermal parameters and complete lists of interatomic distances and angles have been deposited with

the Cambridge Crystallographic Data Centre, 12 Union Road, Cambridge CB2 1EZ, UK. The data are available on request on quoting CCDC-187148.

#### Acknowledgements

This work was supported by the Deutsche Forschungsgemeinschaft, the Fonds der Chemischen Industrie and the Deutscher Akademischer Austauschdienst. We thank The Academy of Finland for generous support.

- 
- [1] H. Schmidbaur, *Gold Bull.* **23**, 11 (1990).  
[2] A. Hyashi, M. M. Olmstead, S. Attar, A. L. Baldi, *J. Am. Chem. Soc. ASAP* (2002).  
[3] P. Pyykkö, J. Li, N. Runeberg, *Chem. Phys. Lett.* **218**, 133 (1994).  
[4] G. Müller, W. Graf, H. Schmidbaur, *Angew. Chem. Int. Ed. Engl.* **27**, 417 (1988).  
[5] P. Pyykkö, *Chem. Rev.* **97**, 597 (1997).  
[6] H. Schmidbaur, *Gold Bull.* **33**, 3 (2000).  
[7] a) V. W. W. Yam, T. F. Lai, C.-M. Che, *J. Chem. Soc., Dalton Trans.* 3747 (1990); b) J. C. Vickery, M. M. Olmstead, E. Y. Fung, A. L. Balch, *Angew. Chem. Int. Ed. Engl.* **36**, 1179 (1997); c) Z. Assefa, B. G. McBurnett, R. J. Staples, J. P. Fackler Jr., B. Assmann, K. Angermaier, H. Schmidbaur, *Inorg. Chem.* **34**, 75 (1995).  
[8] a) H. Schmidbaur, *Chem. Soc. Rev.* 391 (1995); b) D. Braga, F. Grepioni, G. R. Desiraju, *Chem. Rev.* **98**, 1357 (1998).  
[9] T. Mathieson, A. Schier, H. Schmidbaur, *J. Chem. Soc., Dalton Trans.* 1196 (2001).  
[10] W. Schneider, K. Angermaier, A. Sladek, H. Schmidbaur, *Z. Naturforsch.* **51b**, 790 (1996).  
[11] J. D. E. T. Wilton-Ely, H. Ehlich, A. Schier, H. Schmidbaur, *Helv. Chim. Acta* **84**, 3216 (2001).  
[12] T. Mathieson, A. G. Langdon, N. B. Milestone, B. K. Nicholson, *J. Chem. Soc., Dalton Trans.* 201 (1999).  
[13] H. Xiao, K.-K. Cheung, C.-M. Che, *J. Chem. Soc., Dalton Trans.* 3699 (1996).  
[14] S. Ahrland, K. Dreisch, B. Norén, Å. Oscarsson, *Mater. Chem. Phys.* **276**, 281 (1971).  
[15] *MOLPRO*, a package of ab initio programs written by H.-J. Werner and P. J. Knowles, with contributions from R. D. Amos, A. Berning, D. L. Cooper, M. J. O. Deegan, A. J. Dobbyn, F. Eckert, C. Hampel, T. Leininger, R. Lindh, A. W. Lloyd, W. Meyer, M. E. Mura, A. Nicklass, P. Palmieri, K. Peterson, R. Pitzer, P. Pulay, G. Rauhut, M. Schütz, H. Stoll, A. J. Stone, and T. Thorsteinsson (1999).  
[16] D. Andrae, U. Häusserman, M. Dolg, H. Stoll, H. Preuss, *Theor. Chim. Acta* **77**, 123 (1990).  
[17] N. Runeberg, M. Schütz, H.-J. Werner, *J. Chem. Phys.* **110**, 7210 (1999).  
[18] A. Bergner, M. Dolg, W. Kuechle, H. Stoll, H. Preuss, *Mol. Phys.* **80**, 1431 (1993).  
[19] S. Huzinaga, *Gaussian Basis Sets for Molecular Calculations* Amsterdam: Elsevier. (1984).  
[20] T. H. Dunning (Jr.), *J. Chem. Phys.* **90**, 1007 (1989).  
[21] D. Woon, T. H. Dunning Jr., *J. Chem. Phys.* **98**, 1358 (1993).  
[22] G. W. Gokel, R. R. Widera, W. P. Werner, *Org. Synth.* **55**, 96 (1976).  
[23] C. K. Johnson, ORTEP, Report ORNL-5138, Oak Ridge National Laboratory, Oak Ridge, TN, (1976).